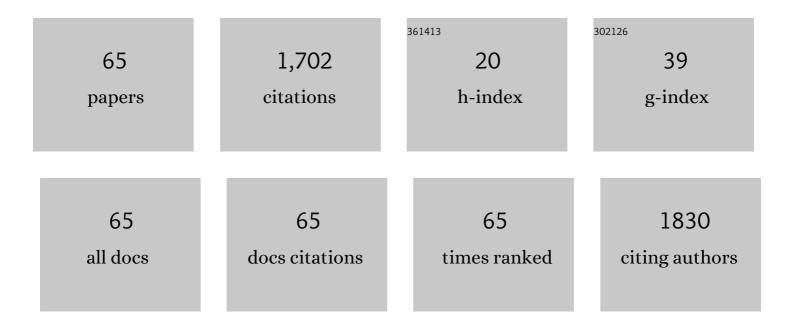
## Ning Wang

List of Publications by Year in descending order

Source: https://exaly.com/author-pdf/9579056/publications.pdf Version: 2024-02-01



#	Article	IF	CITATIONS
1	A highly efficient, in situ wet-adhesive dextran derivative sponge for rapid hemostasis. Biomaterials, 2019, 205, 23-37.	11.4	160
2	Catalytic Activation of H <sub>2</sub> under Mild Conditions by an [FeFe]-Hydrogenase Model via an Active μ-Hydride Species. Journal of the American Chemical Society, 2013, 135, 13688-13691.	13.7	107
3	Reactions of [FeFe]-hydrogenase models involving the formation of hydrides related to proton reduction and hydrogen oxidation. Dalton Transactions, 2013, 42, 12059.	3.3	104
4	Ultrasmall Ru Nanoparticles Highly Dispersed on Sulfur-Doped Graphene for HER with High Electrocatalytic Performance. ACS Applied Materials & Interfaces, 2020, 12, 48591-48597.	8.0	87
5	Carbene–pyridine chelating 2Fe2S hydrogenase model complexes as highly active catalysts for the electrochemical reduction of protons from weak acid (HOAc). Dalton Transactions, 2007, , 1277-1283.	3.3	85
6	Preparation, Facile Deprotonation, and Rapid H/D Exchange of the μ-Hydride Diiron Model Complexes of the [FeFe]-Hydrogenase Containing a Pendant Amine in a Chelating Diphosphine Ligand. Inorganic Chemistry, 2009, 48, 11551-11558.	4.0	84
7	Current progress in interfacial engineering of carbon-based perovskite solar cells. Journal of Materials Chemistry A, 2019, 7, 8690-8699.	10.3	84
8	Hemilabile Bridging Thiolates as Proton Shuttles in Bioinspired H <sub>2</sub> Production Electrocatalysts. Journal of the American Chemical Society, 2016, 138, 12920-12927.	13.7	78
9	A proton–hydride diiron complex with a base-containing diphosphine ligand relevant to the [FeFe]-hydrogenase active site. Chemical Communications, 2008, , 5800.	4.1	73
10	Ru/RuO <sub>2</sub> Nanoparticle Composites with N-Doped Reduced Graphene Oxide as Electrocatalysts for Hydrogen and Oxygen Evolution. ACS Applied Nano Materials, 2020, 3, 12269-12277.	5.0	68
11	Effective wound dressing based on Poly (vinyl alcohol)/Dextran-aldehyde composite hydrogel. International Journal of Biological Macromolecules, 2019, 132, 1098-1105.	7.5	58
12	A multifunctional lipid that forms contrast-agent liposomes with dual-control release capabilities for precise MRI-guided drug delivery. Biomaterials, 2019, 221, 119412.	11.4	53
13	CO-Migration in the Ligand Substitution Process of the Chelating Diphosphite Diiron Complex (μ-pdt)[Fe(CO) <sub>3</sub> ][Fe(CO){(EtO) <sub>2</sub> PN(Me)P(OEt) <sub>2</sub> }]. Inorganic Chemistry, 2008, 47, 6948-6955.	4.0	50
14	Efficient antibacterial dextran-montmorillonite composite sponge for rapid hemostasis with wound healing. International Journal of Biological Macromolecules, 2020, 160, 1130-1143.	7.5	40
15	Intramolecular Iron-Mediated C–H Bond Heterolysis with an Assist of Pendant Base in a [FeFe]-Hydrogenase Model. Journal of the American Chemical Society, 2014, 136, 16817-16823.	13.7	38
16	Photocatalytic Hydrogen Production Based on a Serial Metal alen Complexes and the Reaction Mechanism. ChemCatChem, 2019, 11, 6324-6331.	3.7	25
17	Electrostatic Interactions Accelerating Water Oxidation Catalysis via Intercatalyst O–O Coupling. Journal of the American Chemical Society, 2021, 143, 2484-2490.	13.7	25
18	Redox Reactions of [FeFe]-Hydrogenase Models Containing an Internal Amine and a Pendant Phosphine. Inorganic Chemistry, 2014, 53, 1555-1561.	4.0	24

#	Article	IF	CITATIONS
19	Complexes of MN <sub>2</sub> S <sub>2</sub> ·Fe(η <sup>5</sup> -C <sub>5</sub> R <sub>5</sub> )(CO) as platform for exploring cooperative heterobimetallic effects in HER electrocatalysis. Dalton Transactions, 2017, 46, 5617-5624.	3.3	24
20	A Traceable, Sequential Multistageâ€Targeting Nanoparticles Combining Chemo/Chemodynamic Therapy for Enhancing Antitumor Efficacy. Advanced Functional Materials, 2021, 31, 2101432.	14.9	24
21	A Multifunctional Lipid Incorporating Active Targeting and Dual-Control Release Capabilities for Precision Drug Delivery. ACS Applied Materials & Interfaces, 2020, 12, 70-85.	8.0	21
22	Cyanide-bridged iron complexes as biomimetics of tri-iron arrangements in maturases of the H cluster of the di-iron hydrogenase. Chemical Science, 2016, 7, 3710-3719.	7.4	20
23	Using a novel adsorbent macrocyclic compound cucurbit[8]uril for Pb 2+ removal from aqueous solution. Journal of Environmental Sciences, 2016, 50, 3-12.	6.1	19
24	Supramolecular self-assembly of a [2Fe2S] complex with a hydrophilic phosphine ligand. CrystEngComm, 2008, 10, 267-269.	2.6	18
25	Effect of Bridgehead Steric Bulk on the Intramolecular C–H Heterolysis of [FeFe]-Hydrogenase Active Site Models Containing a P <sub>2</sub> N <sub>2</sub> Pendant Amine Ligand. Inorganic Chemistry, 2016, 55, 411-418.	4.0	17
26	[FeFe]-Hydrogenase active site models with relatively low reduction potentials: Diiron dithiolate complexes containing rigid bridges. Journal of Inorganic Biochemistry, 2008, 102, 952-959.	3.5	16
27	Seamless Interfacial Formation by Solution-Processed Amorphous Hydroxide Semiconductor for Highly Efficient Electron Transport. ACS Applied Energy Materials, 2018, 1, 4564-4571.	5.1	16
28	Engineering heterostructure and crystallinity of Ru/RuS2 nanoparticle composited with N-doped graphene as electrocatalysts for alkaline hydrogen evolution. Chinese Chemical Letters, 2021, 32, 3591-3595.	9.0	16
29	Zinc(II)porphyrin-Based Porous Ionic Polymers (PIPs) as Multifunctional Heterogeneous Catalysts for the Conversion of CO <sub>2</sub> to Cyclic Carbonates. Industrial & Engineering Chemistry Research, 2022, 61, 5093-5102.	3.7	16
30	The influence of a S-to-S bridge in diiron dithiolate models on the oxidation reaction: a mimic of the Hairox state of [FeFe]-hydrogenases. Chemical Communications, 2014, 50, 9255-9258.	4.1	15
31	Synthesis, protonation and electrochemical properties of trinuclear NiFe2 complexes Fe2(CO)6(l¼3-S)2[Ni(Ph2PCH2)2NR] (R=n-Bu, Ph) with an internal pendant nitrogen base as a proton relay. Inorganica Chimica Acta, 2009, 362, 372-376.	2.4	14
32	The antimicrobial activities of a series of bis-quaternary ammonium compounds. Chinese Chemical Letters, 2011, 22, 887-890.	9.0	14
33	A traceable, CSH/pH dual-responsive nanoparticles with spatiotemporally controlled multiple drugs release ability to enhance antitumor efficacy. Colloids and Surfaces B: Biointerfaces, 2021, 205, 111866.	5.0	14
34	Orthogonal Supramolecular Assembly Triggered by Inclusion and Exclusion Interactions with Cucurbit[7]uril for Photocatalytic H 2 Evolution. ChemSusChem, 2020, 13, 394-399.	6.8	13
35	Cycloaddition Reactions of Epoxides and CO <sub>2</sub> by the Novel Imidazoliumâ€Functionalized Metalloporphyrins: Optimization and Analysis using Response Surface Methodology. ChemCatChem, 2020, 12, 4839-4844.	3.7	13
36	Pyridiniumâ€functionalized metalloporphyrins as bifunctional catalysts for cycloaddition of epoxides and carbon dioxide. Applied Organometallic Chemistry, 2020, 34, e5382.	3.5	11

#	Article	IF	CITATIONS
37	Covalent Metalloporphyrin Polymer Coated on Carbon Nanotubes as Bifunctional Electrocatalysts for Water Splitting. Inorganic Chemistry, 2022, 61, 10198-10204.	4.0	11
38	Endogenous reactive oxygen species burst induced and spatiotemporally controlled multiple drug release by traceable nanoparticles for enhancing antitumor efficacy. Biomaterials Science, 2021, 9, 4968-4983.	5.4	10
39	Photo(electro)catalytic activity enhancement of PhC <sub>2</sub> Cu by Fe doping induced energy band modulation and luminescence chromism switching. Catalysis Science and Technology, 2021, 11, 2379-2385.	4.1	10
40	An MRI-guided targeting dual-responsive drug delivery system for liver cancer therapy. Journal of Colloid and Interface Science, 2021, 603, 783-798.	9.4	10
41	A zinc porphyrin polymer as efficient bifunctional catalyst for conversion of CO <sub>2</sub> to cyclic carbonates. Applied Organometallic Chemistry, 2022, 36, .	3.5	10
42	Pseudopolyrotaxanes of Cucurbit[6]uril: A Threeâ€Dimensional Network Selfâ€assembled by ClO <sub>4</sub> <sup>â^'</sup> (H <sub>2</sub> O) <sub>2</sub> Water Clusters. Chinese Journal of Chemistry, 2012, 30, 941-946.	4.9	9
43	Synthesis and characterization of porphyrin-based porous coordination polymers obtained by supercritical CO2 extraction. Journal of Materials Science, 2018, 53, 10534-10542.	3.7	9
44	Synthesis and evaluation of mono- and multi-hydroxyl low toxicity pH-sensitive cationic lipids for drug delivery. European Journal of Pharmaceutical Sciences, 2019, 133, 69-78.	4.0	9
45	Magnetic Resonance Imaging-Guided Multi-Stimulus-Responsive Drug Delivery Strategy for Personalized and Precise Cancer Treatment. ACS Applied Materials & Interfaces, 2021, 13, 50716-50732.	8.0	9
46	Sensitive and precise visually guided drug delivery nanoplatform with dual activation of pH and light. Acta Biomaterialia, 2022, 141, 374-387.	8.3	9
47	Protophilicity, electrochemical property, and desulfurization of diiron dithiolate complexes containing a functionalized C2 bridge with two vicinal basic sites. Polyhedron, 2009, 28, 1138-1144.	2.2	8
48	Preparation, characterization and catalytic oxidation properties of silica composites immobilized with cationic metalloporphyrins. Journal of Materials Science, 2018, 53, 14241-14249.	3.7	6
49	Meshless Method for Nonuniform Heat-Transfer/Solidification Behavior of Continuous Casting Round Billet. Metallurgical and Materials Transactions B: Process Metallurgy and Materials Processing Science, 2020, 51, 236-246.	2.1	6
50	A Benzimidazoleâ€ <b>l</b> inked Porphyrin Covalent Organic Polymers as Efficient Heterogeneous Catalyst/Photocatalyst. Applied Organometallic Chemistry, 0, , .	3.5	6
51	Triple-responsive targeted hybrid liposomes with high MRI performance for tumor diagnosis and therapy. Materials Chemistry Frontiers, 2021, 5, 6226-6243.	5.9	5
52	Precise delivery of multi-stimulus-responsive nanocarriers based on interchangeable visual guidance. Materials Science and Engineering C, 2021, , 112558.	7.3	5
53	Halideâ€Anion Water Clusters in Cucurbit[6]uril Supramolecular Systems. Chinese Journal of Chemistry, 2016, 34, 1114-1120.	4.9	4
54	Synthesis, structure and electrocatalytic H2-evoluting activity of a dinickel model complex related to the active site of [NiFe]-hydrogenases. Chinese Chemical Letters, 2020, 31, 2483-2486.	9.0	4

#	Article	IF	CITATIONS
55	Synthesis of Mn (III)–porphyrin porous coordination polymers as heterogeneous catalysts for CO 2 cycloaddition reaction. Applied Organometallic Chemistry, 2021, 35, e6228.	3.5	4
56	Modeling of capacitively coupled contactless conductivity detection on microfluidic chips. Microsystem Technologies, 2013, 19, 1991-1996.	2.0	3
57	Metalloporphyrinsâ€Al <sup>3+</sup> porous coordination polymers: Preparations, Characterizations and Catalytic Properties. Applied Organometallic Chemistry, 2019, 33, e5055.	3.5	3
58	Molecular Cobalt Catalysts Grafted onto Polymers for Efficient Hydrogen Generation Cathodes. Solar Rrl, 2021, 5, 2000281.	5.8	3
59	Chloridobis(dimethylglyoximato-κ2N,N′)(ethyl pyridine-4-carboxylate-κN)cobalt(III) chloroform monosolvate. Acta Crystallographica Section E: Structure Reports Online, 2012, 68, m204-m205.	0.2	1
60	Study of factors influencing the fabrication of Coâ€porphyrin porous coordination polymer via metal–organic gel intermediate. Applied Organometallic Chemistry, 2019, 33, e5215.	3.5	1
61	Bioinspired Design of Positioned Amine Assists Hydrogen Evolution from Neutral Water by Nickel Tripyridineâ€Điamine. ChemCatChem, 2020, 12, 3853-3856.	3.7	1
62	Introducing electrostatic interaction into Ru(bda) complexes for promoting water-oxidation catalysis. Journal of Molecular Structure, 2021, 1242, 130745.	3.6	1
63	Polydopamine Decorated Ru-Ni(OH)2 Nanosheets for Enhanced Performance of Hydrogen Evolution in Alkaline Media. Catalysis Letters, 0, , 1.	2.6	1
64	Chloridobis(dimethylglyoximato-κ2N,N′)(ethyl pyridine-3-carboxylate-κN)cobalt(III). Acta Crystallographica Section E: Structure Reports Online, 2012, 68, m20-m20.	0.2	0
65	Effect of the NiN2S2 Metallothiolate Ligands on the Preparation, Structure, and Property of Dinickel Complexes Related to [NiFe]-Hydrogenases Active Site. Catalysis Letters, 2022, 152, 98-105.	2.6	Ο